

Biofabrication



PAPER

Anisotropic poly (glycerol sebacate)-poly (ϵ -caprolactone) electrospun fibers promote endothelial cell guidance

Akhilesh K Gaharwar^{1,2,3,4,9,10}, Mehdi Nikkha^{3,4,9,11}, Shilpa Sant^{5,6,7} and Ali Khademhosseini^{2,3,4,8}

¹ David H Koch Institute for Integrative Cancer Research, Massachusetts Institute of Technology, Cambridge, MA 02139, USA

² Wyss Institute for Biologically Inspired Engineering, Harvard University, Boston, MA 02115, USA

³ Center for Biomedical Engineering, Department of Medicine, Brigham and Women's Hospital, Harvard Medical School, Cambridge, MA 02139, USA

⁴ Harvard-MIT Division of Health Sciences and Technology, Massachusetts Institute of Technology, Cambridge, MA 02139, USA

⁵ Department of Pharmaceutical Sciences, School of Pharmacy, University of Pittsburgh, Pittsburgh, PA 15261, USA

⁶ Department of Bioengineering, Swansea School of Engineering, University of Pittsburgh, Pittsburgh, PA 15261, USA

⁷ McGowan Institute for Regenerative Medicine, University of Pittsburgh, Pittsburgh, PA 15219, USA

⁸ Department of Physics, King Abdulaziz University, Jeddah, Saudi Arabia

⁹ Contributed equally.

¹⁰ Currently at the Department of Biomedical Engineering and Department of Materials Science & Engineering, Texas A&M University, College Station, TX 77841, USA.

¹¹ Currently at Harrington Department of Biomedical Engineering, School of Biological and Health Systems Engineering, Arizona State University, Tempe, AZ 85287, USA.

E-mail: shs149@pitt.edu and alik@rics.bwh.harvard.edu

Keywords: electrospun scaffolds, tissue engineering, poly (glycerol sebacate), endothelial cells

Abstract

Topographical cell guidance is utilized to engineer highly organized and aligned cellular constructs for numerous tissue engineering applications. Recently, electrospun scaffolds fabricated using poly(glycerol sebacate) (PGS) and poly(ϵ -caprolactone) (PCL) have shown a great promise to support valvular interstitial cell functions for the development of tissue engineered heart valves. However, one of the major drawbacks of PGS-PCL scaffolds is the lack of control over cellular alignment. In this work, we investigate the role of scaffold architecture on the endothelial cell alignment, proliferation and formation of organized cellular structures. In particular, PGS-PCL scaffolds with randomly oriented and highly aligned fibers with tunable mechanical properties were fabricated using electrospinning technique. After one week of culture, endothelial cells on the aligned scaffolds exhibited higher proliferation compared to those cultures on randomly oriented fibrous scaffolds. Furthermore, the endothelial cells reorganized in response to the topographical features of aligned scaffolds forming highly organized cellular constructs. Thus, topographical contact guidance, provided by aligned PGS-PCL scaffolds, is envisioned to be useful in developing cellular structures for vascular tissue engineering.

1. Introduction

Polyglycerol sebacate (PGS), a biodegradable elastomer, has been extensively evaluated for a broad range of applications in regenerative medicine including cardiovascular patches (Chen *et al* 2008), vascular tissue grafts (Motlagh *et al* 2006), engineered heart valves (Masoumi *et al* 2013), cartilage tissues (Kempainen and Hollister 2010), nerve conduits (Sundback *et al* 2005), retinal implants (Pritchard *et al* 2010), and surgical sealants (Chen *et al* 2011). Such diverse applications are primarily attributed to the controlled degradation profile, non-toxic byproducts and highly

elastomeric nature of PGS (Rai *et al* 2012, Wang *et al* 2003, Wang *et al* 2002). In addition, the surface erodible characteristic of PGS makes it desirable to develop scaffolds for tissue engineering applications (Wang *et al* 2002, Jaafar *et al* 2010, Sun *et al* 2011, Sun *et al* 2009, Chen *et al* 2008). In the body, the cellular microenvironment, exhibits a complex milieu of biophysical and biochemical signals, which play a crucial role in directing cellular functions. For example, extracellular matrix (ECM) proteins as well as the basement membrane are comprised of heterogeneous mixture of pores, ridges and fibers at micro and nano-scale levels, which act as a scaffold to guide various cell

functions (Sant *et al* 2012, Dolatshahi-Pirouz *et al* 2014, Gaharwar *et al* 2014a). Such topographical features continuously interact with the cells and influence their physiological function via cell-matrix signaling pathways (Chen *et al* 2004, Stevens and George 2005, Kulangara and Leong 2009, Nikkhah *et al* 2012a, Gaharwar *et al* 2014b).

To date, micro- and nanofabrication techniques have been utilized to develop scaffolds with well-defined topographical features to mimic native tissue architecture at different length scales (Gaharwar *et al* 2014b, Khademhosseini *et al* 2006, Zorlutuna *et al* 2012, Mihaila *et al* 2013). For example, in a recent study micromolding technique was used to develop PGS scaffolds with diamond-shaped pores that resulted in anisotropic mechanical properties of the scaffolds (Engelmayr *et al* 2008, Masoumi *et al* 2013). In particular, the importance of designing scaffolds with anisotropic structure was underlined by growing evidence that scaffolds with structural anisotropy play a major role in guiding cellular behaviors. In another work, a PGS scaffold with accordion-like honeycomb structures was fabricated to promote the formation of aligned cellular constructs (Engelmayr *et al* 2008). Specifically, the anisotropic structure and directionally dependent mechanical properties were utilized as guidance cues to regulate cell adhesion, shape, spreading, and migration.

In the past few years, electrospinning has become a popular approach to fabricate highly porous tissue engineering scaffolds to mimic the natural ECM microenvironment (Bhardwaj and Kundu 2010, Gaharwar *et al* 2014a, Fleischer and Dvir 2012, Gaharwar *et al* 2014b). For instance, in a recent study, injectable nanofibers of PGS were fabricated to engineer cardiac tissues (Ravichandran *et al* 2012). In the proposed approach, a co-axial electrospinning setup was utilized to fabricate scaffolds from PGS and poly-L-lactic acid (PLLA). PLLA was later removed to obtain injectable PGS fibers for minimally invasive therapies. Interestingly, cardiac markers including connexin 43, actinin, troponin, and myosin heavy chain were highly expressed in PGS nanofibers compared to PLLA (Ravichandran *et al* 2012). To further enhance physical, chemical and biological functionality, PGS has been blended or copolymerized with a range of natural and synthetic polymers (Ravichandran *et al* 2011, Ifkovits *et al* 2009, Sant *et al* 2011, Tong *et al* 2011, Kharaziha *et al* 2013). For example, PGS-PEG block copolymers were synthesized with different mechanical properties ranging from soft elastomers to mechanically stiff in order to mimic properties of soft tissues such as cartilage, cardiac tissues, vocal cords (Zhang *et al* 2013). In another study, a wide range of mechanical properties of electrospun PGS-gelatin scaffolds was obtained through changing the ratio of PGS and gelatin (Ifkovits *et al* 2009, Kharaziha *et al* 2013). Modulating the acrylation degree of PGS was also used to alter the degradation profile and

mechanical properties of PGS scaffolds for myocardial infarction therapy (Ifkovits *et al* 2009). Recently, blend of PGS with poly(ϵ -caprolactone) (PCL), a semi-crystalline polyester, was used to develop scaffolds that mimic the mechanical properties of native heart valves. (Sant *et al* 2011, Sant *et al* 2013). The fibrous PGS-PCL scaffolds supported spreading and proliferation of human umbilical vein endothelial cells (HUVECs) and fibroblastic differentiation of mesenchymal stem cells (MSCs) (Sant *et al* 2011, Tong *et al* 2011). In particular, by controlling the amount of PGS and PCL, it was possible to tailor the degradation rate of the scaffolds to match that of ECM secretion by valvular interstitial cells (VICs) (Sant *et al* 2011, Sant *et al* 2013). However, one of the limitations of the previously developed PGS-PCL electrospun scaffolds was the lack of control over the structural anisotropy of the construct and subsequent cellular alignment (Sant *et al* 2011, Sant *et al* 2013). Moreover in a recent study, it was observed that anisotropic structures are promising candidates for valve tissue engineering, as VICs proliferate and form aligned structure in anisotropic scaffolds (Sohier *et al* 2014). Therefore, we hypothesized that by controlling the fiber orientation, anisotropy can be incorporated within the fibrous scaffolds to provide topological cues for enhanced cellular signaling.

In this study, we investigated the effect of PGS-PCL fiber organization on endothelial cells behavior. Electrospinning was used to fabricate random and aligned scaffolds from blends of PGS and PCL polymers with tunable mechanical properties. The effect of fiber orientation was evaluated on endothelial cell attachment, proliferation and organization. The specific goal of this project is to investigate the potential applicability of PGS-PCL fibrous scaffolds for engineering vascularized tissue substitutes. We hypothesize that the anisotropic PGS-PCL scaffolds will assist in formation of aligned structure, mimicking native tissue architecture, to develop small and medium-sized tissue engineered vascular grafts.

2. Experimental section

2.1. Materials

PGS (Molecular weight $\sim 5,012$ Da and PDI ~ 2.64) was synthesized according to previously published polycondensation methods (Wang *et al* 2003, Zhang *et al* 2013). Briefly, equimolar glycerol (Sigma-Aldrich, USA) and sebacic acid (Sigma-Aldrich) were heated to 130 °C for 2 h under Argon gas in a round bottom reactor. The pressure was gradually decreased to 50 mTorr and the reaction was continued under vacuum condition for 48 h. PCL ($C_6H_{10}O_2$)_n (Molecular weight 70–90 kDa) was obtained from Sigma-Aldrich (USA).

2.2. Scaffold fabrication

The electrospun scaffolds were fabricated by first dissolving PCL (10% w/v) and PGS (5% w/v) in 9:1 ratio of anhydrous chloroform and ethanol according to previously published methods (Sant *et al* 2011, Sant *et al* 2013). Electrospinning of the PGS-PCL mixture was carried out using a blunt needle (21G), 2 mL h⁻¹ flow rate, 12.5 kV (Glassman High Voltage, USA) and 18 cm distance between the collector and needle. Random scaffolds were obtained by using a circular aluminum collector plate (eight inches in diameter) while aligned scaffolds were fabricated by using a parallel collector plate (five inches in length with a gap of one inch). The voltage and distance were kept constant to obtain random and aligned scaffolds. The fabricated electrospun scaffolds were dried in vacuum overnight to remove the residual solvent.

2.3. Microstructure evaluation

Electrospun fiber structure and morphology was evaluated by scanning electron microscopy (SEM) (JSM 5600LV, JEOL, USA). The fabricated scaffolds were coated with Au/Pd for 2 min using a Hummer 6.2 sputter coater (Ladd Research, USA). SEM images were acquired at 5 KV accelerating voltage, 5 mm working distance and a spot size of 20. The images were analyzed using Image J (NIH, USA) software and fiber diameter was calculated from at least 100 fibers. The alignment of fibers was characterized using directional plugin of ImageJ to obtain fast Fourier transformation (FFT) of SEM images.

2.4. Chemical characterization

Fourier transform infrared (FTIR) spectra of the fabricated electrospun scaffolds were obtained using Alpha FTIR spectrometer (Bruker, USA). For each sample, at least 24 scans with 4 cm⁻¹ resolution were collected. Thermal properties of PGS-PCL scaffolds were determined by differential scanning calorimeter (DSC) 8500 (Perkin-Elmer, USA). Pre-weighted scaffolds were sealed in aluminum pans and were heated at 10 °C min⁻¹. The samples were then subjected to two heating and cooling cycles between -70 °C to 150 °C under nitrogen gas. The second heating cycle was used to determine the melting temperature (T_m) and the melting enthalpy (ΔH_m).

2.5. Mechanical testing

The mechanical properties of the blended PGS-PCL scaffolds were characterized using Instron 5943 Materials Testing System (Instron, USA) at 10 mm min⁻¹ strain rate with 50 N load cell. The scaffolds were cut in rectangular shapes (10 × 5 mm²) with approximate thickness of 100–140 μm. For the tensile test, samples were gripped from two end using rubber gripped to avoid slippage. A preload of 0.01 N was applied on the scaffolds before the start of the experiment. The elastic modulus was calculated from the linear section of

stress-strain curve within 5–15% strain range. The morphology of electrospun scaffolds was evaluated after the mechanical deformation using SEM imaging. The fractured samples were coated with Au/Pd before the imaging to determine the effect of mechanical deformation on topography.

2.6. Cell seeding and proliferation

GFP-expressing HUVECs (passage ~10–15) were used in this work. The cells were cultured in endothelial specific growth medium (EGM-2, Lonza, USA) containing 2% fetal bovine serum, human fibroblast growth factor, vascular endothelial growth factor, human epidermal growth factor, insulin growth factor (R3-IGF-I), ascorbic acid, hydrocortisone, heparin, and 1% gentamicin and amphotericin B. The fibrous scaffolds (5 × 5 mm²) were sterilized using 70% ethanol and the cells were seeded on each scaffold with a density of 2 × 10⁵ cells in ultra-low adhesion plates. The effect of fiber orientation on the metabolic activity of the cells was evaluated using Alamar Blue assay (Invitrogen, USA) over a period of seven days.

2.7. Histology

Cell-seeded scaffolds were fixed using 4% paraformaldehyde (PF) solution and then dehydrated using an alcohol gradient and paraffin-embedding. The fixed samples were then sectioned (10 μm) and mounted on glass slides and washed in xylene. The sections were finally rehydrated before staining with hemotoxylin and eosin (H&E).

2.8. Cellular alignment analysis

After seven days of culture, the cell-seeded scaffolds were fixed in 4% PF solution and cell nuclei were stained with 4', 6-diamidino-2-phenylindole (DAPI). The confocal images were obtained using inverted laser scanning confocal microscope (SP5 X MP, Leica). The 3D projected image was obtained using Leica application suite (LAS) software by stacking the acquired confocal images using Imaris software (Bitplane, Zurich, Swiss). The nuclei alignment was determined according to our previously published protocols (Nikkhah *et al* 2012b).

2.9. Immunofluorescence

Actin cytoskeleton organization and endothelial cell specific intercellular junction marker (CD31) expression were evaluated using confocal microscopy on the random and aligned scaffolds. Cell-seeded scaffolds were fixed in 4% PF solution and the cell membrane was permeabilized using 0.1% Triton X-100 for 30 min. Subsequently, the samples were blocked in 1% bovine serum albumin (BSA) for actin cytoskeleton and in 10% horse serum for CD-31 staining, respectively. Actin filaments were stained using 1:40 dilution of Alexa Fluor-594 phalloidin (Abcam) in 0.1% BSA, while CD-31 staining was performed using 1:100

dilution of monoclonal mouse anti-CD31 primary antibody (Abcam) and 1:200 dilution of Alexa Fluor-594 conjugated goat anti-mouse secondary antibody in 10% horse serum.

2.10. Statistical analysis

All experimental data were presented as mean \pm standard deviation (SD). Student's *t*-test was used to analyze the differences between the groups for structural analysis and mechanical testing ($*p < 0.05$).

3. Results and discussion

Both, PGS and PCL are considered as aliphatic polyesters. PGS is an amorphous polymer at room temperature and has a faster *in vivo* degradation rate compared to PCL (Wang *et al* 2003, Sundback *et al* 2005). Alternatively, PCL is a semi-crystalline polymer, which slowly degrades over a period of 2–4 years depending on its specific properties (i.e. molecular weight and crystallinity) (Lam *et al* 2008). Through blending PGS and PCL, it is possible to develop hybrid biomaterials resembling the natural ECM architecture with a broad spectrum of mechanical properties and degradation profiles to modulate various cell functions (Sant *et al* 2011, Sant *et al* 2013). Due to their unique property combinations, PGS-PCL based electrospun scaffolds can be extensively used for cardiovascular tissue engineering applications (i.e. heart valves, vascular grafts).

3.1. Structural and chemical characterization of electrospun scaffolds

The fiber morphology of random and aligned scaffolds was determined using SEM imaging (figure 1(a)). Both random and aligned scaffold exhibited fibers with uniform and smooth surface morphology with diameter in the range of $3.4 \pm 0.78 \mu\text{m}$ and $4.7 \pm 0.6 \mu\text{m}$, respectively. The microscopic images indicated enhanced fiber orientation within the aligned scaffolds compared to the random ones. To further analyze the degree of alignment, we performed two-dimensional (2D) FFT of the SEM images. We first converted the spatial organization of fibers into a mathematically defined frequency domain. This process maps the rate of change of intensities across the original images and the output image depicts the orientation of the object in the original image. The 2D FFT images (figure 1(a)) indicated that the random scaffolds comprised of fibers with a small degree of orientation. Alternatively, aligned scaffold exhibited highly oriented structure as indicated by an intense peak perpendicular to the fiber orientation.

The preferred orientation of fibers within aligned and random scaffolds was also investigated using ImageJ software (Directional plugin). The results indicated relatively flat and skewed histogram for random and normal distribution comprised of a sharp peak

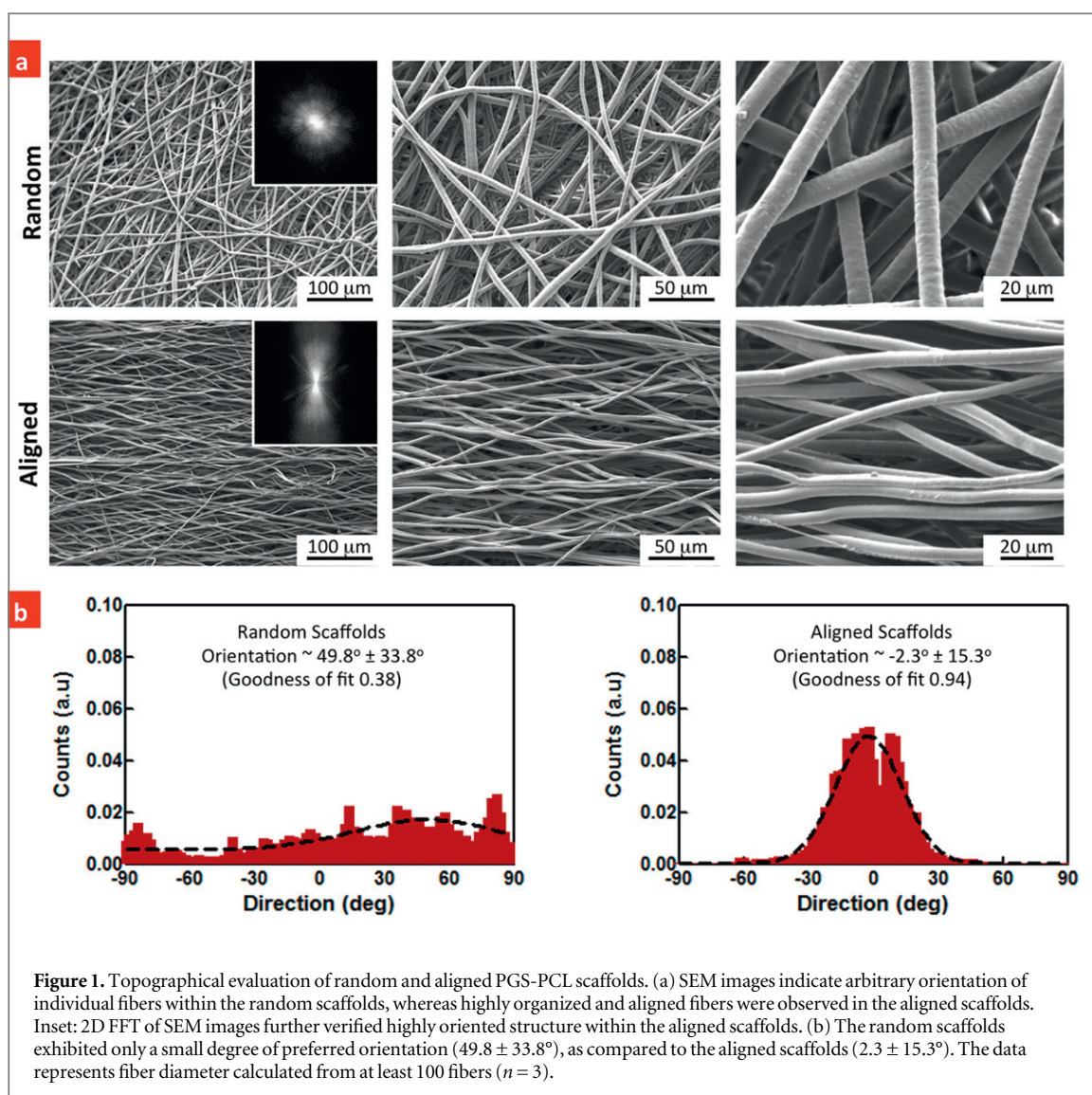
within the aligned scaffolds. The fitting data indicated a small degree of preferred orientation in the random scaffolds at $49.8 \pm 33.8^\circ$ (goodness of fit = 0.38). On the other hand, preferred orientation was $-2.3 \pm 15.3^\circ$ within the aligned scaffolds (goodness of fit = 0.94) (figure 1(b)). The goodness of the fit indicated that the aligned scaffolds had almost 94% of the fibers in the range of $-2.3 \pm 15.3^\circ$. In the current study, we selected only random and highly aligned scaffold, however there are range of parameters in electrospinning processes that can be tuned to obtain variable degree of fiber alignment (Courtney *et al* 2006).

FTIR spectroscopy was performed to determine the presence of PGS and PCL within electrospun scaffolds. Both PCL and PGS showed very similar IR bands at 2923 cm^{-1} (CH_2 stretching-asymmetric), 2857 cm^{-1} (CH_2 stretching-symmetric), 1293 cm^{-1} (C–O and C–C stretching in the crystalline phase), 1720 cm^{-1} (carbonyl stretching) and 1240 cm^{-1} (C–O–C stretching-asymmetric) (figure 2(a)). Additionally, PGS showed an additional hydroxyl peak at 3500 cm^{-1} , which was not observed in pure PCL. Overall, electrospun PGS-PCL scaffolds showed both PGS and PCL peaks, indicating composite structure of the fibers.

We further used DSC to determine the effect of addition of PGS on the thermal properties of the electrospun PGS-PCL scaffolds. Figure 2(b) shows the DSC thermograms (heating cycles) of PGS, PCL and PGS-PCL scaffolds. The melting temperature (T_m) of pure PCL and pure PGS was calculated to be 57.8°C and 12.4°C while the melting enthalpy (ΔH) was found to be 47.96 J g^{-1} and 1.72 J g^{-1} , respectively. Notably, electrospun scaffolds, exhibited two distinct T_m (56.1 and 11.9°C) indicating presences of both PGS and PCL within the blended scaffolds. The presence of two distinct peaks indicates that PGS and PCL are not fully miscible and phase separation might occur after the electrospinning process. These results were in agreement with the previously published reports (Bolgen *et al* 2005, Cai and Liu 2008, Liu *et al* 2007).

3.2. Effect of electrospun fiber orientation on mechanical properties of scaffolds

The mechanical properties of biomaterials are among crucial parameters, which significantly influence cell functions. In particular, previous studies have demonstrated that scaffolds with low stiffness result in cells with round morphology, while scaffolds with high stiffness will lead to stretched and spindle like cellular morphology (Engler *et al* 2006). On the other hand, organs and tissues within the body exhibit different mechanical properties depending on their functionality. For instance, vascular system undergoes continuous cyclic mechanical deformation, exhibits elastic modulus in the range of 2.25–130 MPa depending on the physiological anatomy, location and functionality of the blood vessel (Hasan *et al* 2014, Sacks *et al* 2009,

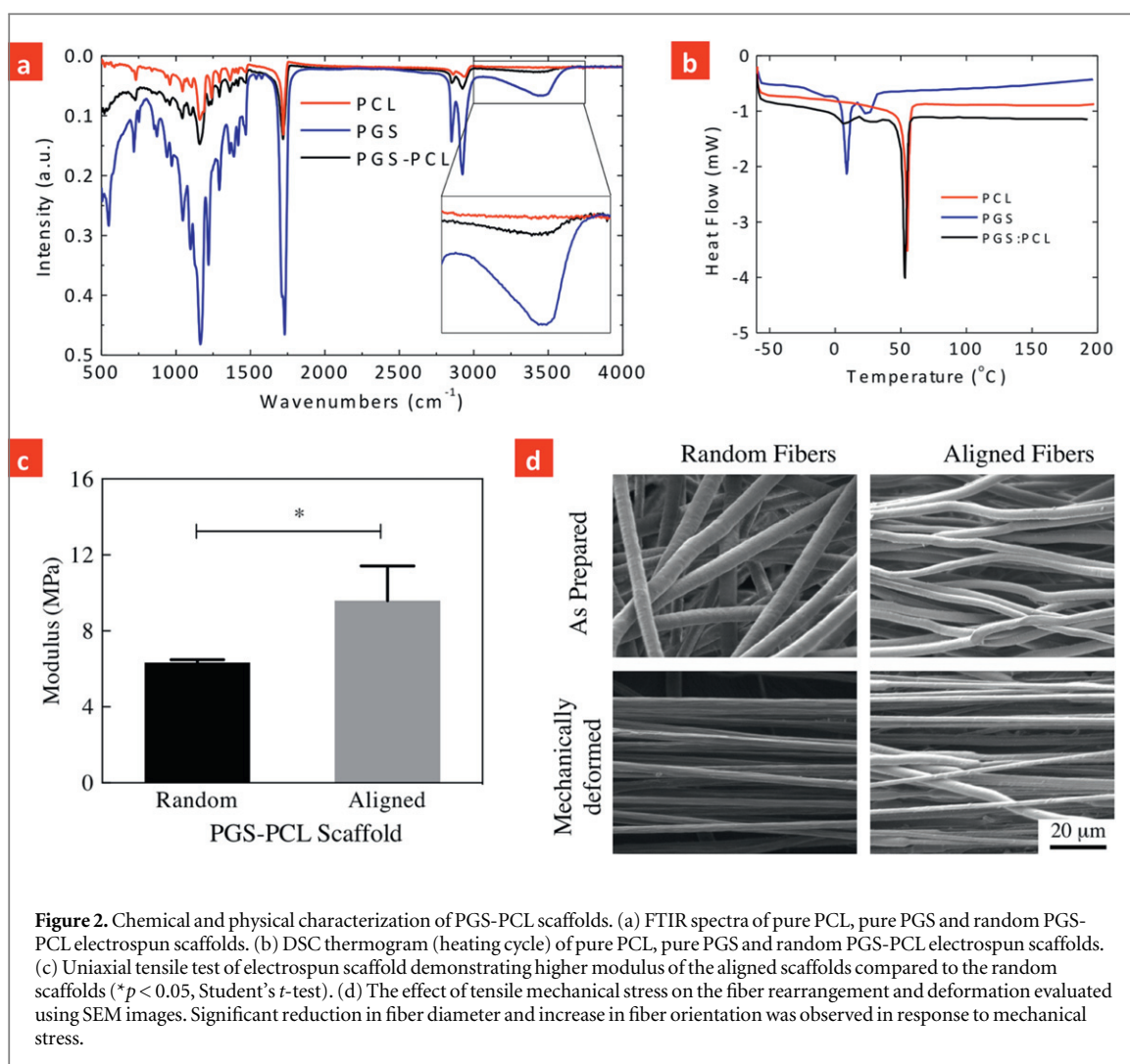


Wagenseil and Mecham 2009). Therefore, we investigated the mechanical properties of fibrous scaffolds using uniaxial tensile test (performed horizontal to the direction of the aligned fibers) (figure 2(c)). The results indicated that random and aligned PGS-PCL scaffolds exhibited elastic modulus of 6.3 ± 0.1 MPa and 9.6 ± 1.1 MPa, respectively ($*p < 0.05$, Student's *t*-test). It is anticipated that the increase in the mechanical strength of the aligned scaffolds may be due to the oriented architecture of the scaffold, which is capable of bearing a higher load compared to the random scaffolds. Under mechanical stress, during initial loading process, fibrous scaffolds undergo fiber rearrangement before the mechanical deformation of individual fibers. In case of aligned scaffolds, this process shortens as most of the fibers are aligned and significant fiber rearrangement is not required. Due to such behavior, the modulus of aligned scaffolds was significantly higher compared to the random scaffolds.

Our mechanical testing results are in agreement with previously published results (Sant *et al* 2011, Sant

et al 2013). Both PCL and PGS-PCL scaffolds have shown to have modulus around 7–8 MPa (Sant *et al* 2011, Sant *et al* 2013). The addition of PGS to PCL did not result in any significant change in mechanical properties. However, alignment of fibers has shown to have significant effect on the mechanical stiffness of PCL scaffolds (Baker *et al* 2008). For example, aligned PCL scaffolds have two-fold higher modulus compared to random scaffolds (Baker *et al* 2008). However, such a dramatic increase in modulus was not observed in PGS scaffolds. Such behavior might be attributed to the presence of PGS that resulted in phase separation from PCL upon electrospinning. This is further supported by the DSC data where two distinct peaks for PGS and PCL were observed.

The effect of mechanical deformation on microstructure was evaluated further using SEM imaging. Figure 2(d) compares the microstructure of random and aligned scaffolds before and after mechanical deformation. In random scaffolds, mechanical deformation resulted in a decrease in fiber diameter from 4.7 ± 0.6 μm to 2.6 ± 0.2 μm , and significant fiber



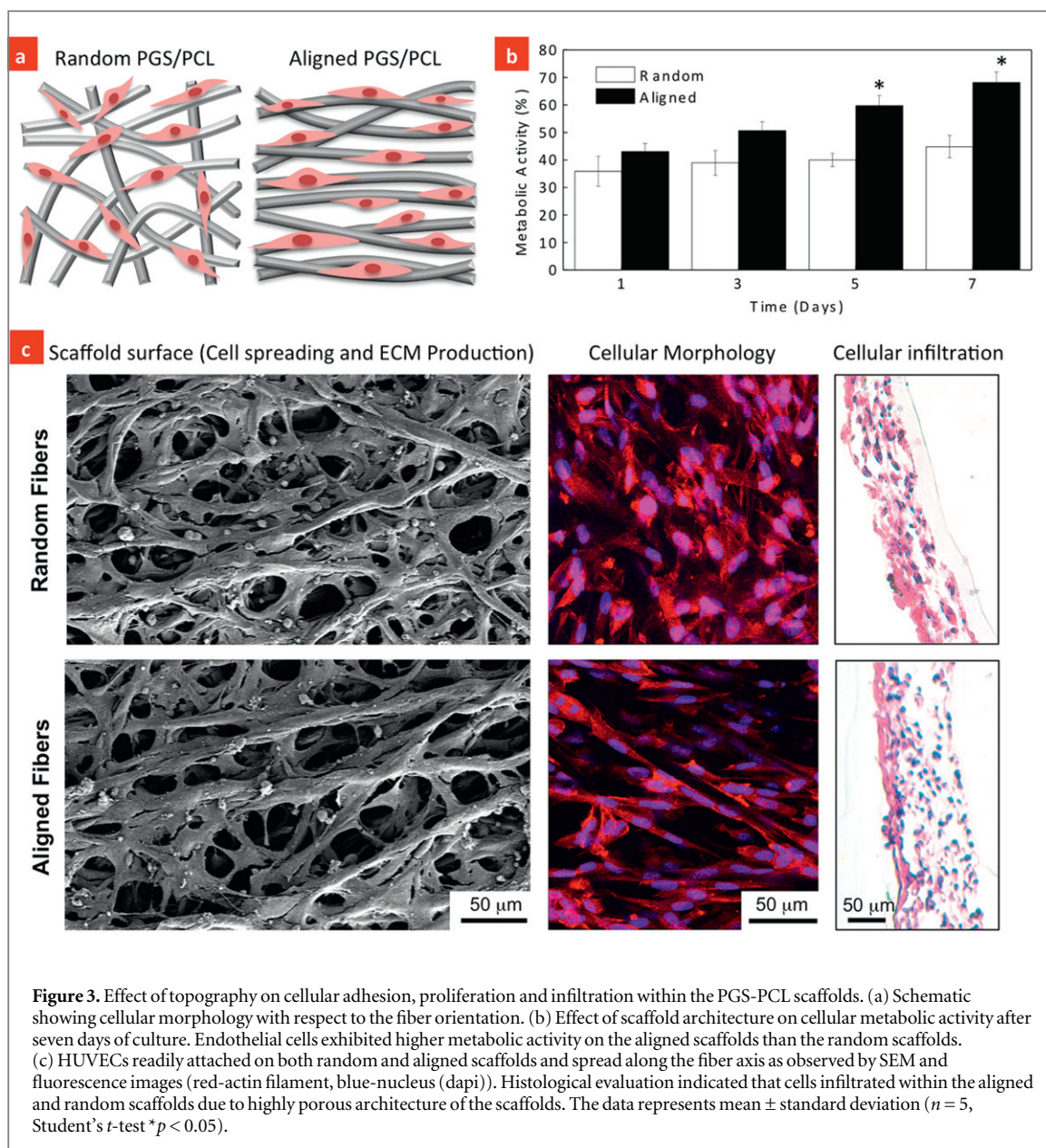
alignment. The deformed fibers showed uniform and smooth surface morphology. Alternatively, within aligned scaffolds, the mechanical deformation resulted in a decrease in fiber diameter from $3.2 \pm 0.8 \mu\text{m}$ to $1.5 \pm 0.5 \mu\text{m}$. The deformed fibers showed necking behavior in the aligned scaffolds.

3.3. Effect of electrospun fiber orientation on cell spreading and proliferation

Earlier studies have reported that electrospun PGS-PCL scaffolds promote cell adhesion and proliferation compared to PCL scaffolds (Sant *et al* 2011), mainly due to their enhanced hydrophilicity compared to hydrophobic PCL scaffolds (Sant *et al* 2011). Herein, the effect of random and aligned scaffolds on endothelial cells adhesion and spreading was investigated (figure 3(a)). The effect of fiber orientation on the metabolic activity of HUVECs was investigated using Alamar Blue assay. The metabolic activity of HUVECs seeded on the aligned scaffolds was higher compared to the random scaffolds (figure 3(b)). In particular, aligned scaffolds induced higher metabolic activity toward the formation of a confluent monolayer over a longer period of culture time (i.e. day seven).

SEM images clearly demonstrated that HUVECs adhered and spread on both, random and aligned scaffolds suggesting the dominance of material properties over structural (fiber organization) cues on cellular attachment (figure 3(c)). On the aligned scaffolds, the cells exhibited spindle-like morphology and were highly organized and elongated along the fiber direction. Alternatively, the cells demonstrated stellate-shape morphology and were distributed in different directions as well as in between the neighboring fibers on the random scaffolds. Fluorescence images shown in figure 3(c) were in agreement with SEM images confirming that the cells extended their cytoskeletal structure in a direction parallel to the electrospun fibers on the aligned scaffolds. Furthermore, the histological sections of the scaffolds confirmed homogeneous penetration and uniform migration of the cells within the interior of regions of the electrospun scaffolds due to highly porous architecture of the scaffolds (figure 3(c)) irrespective of their alignment.

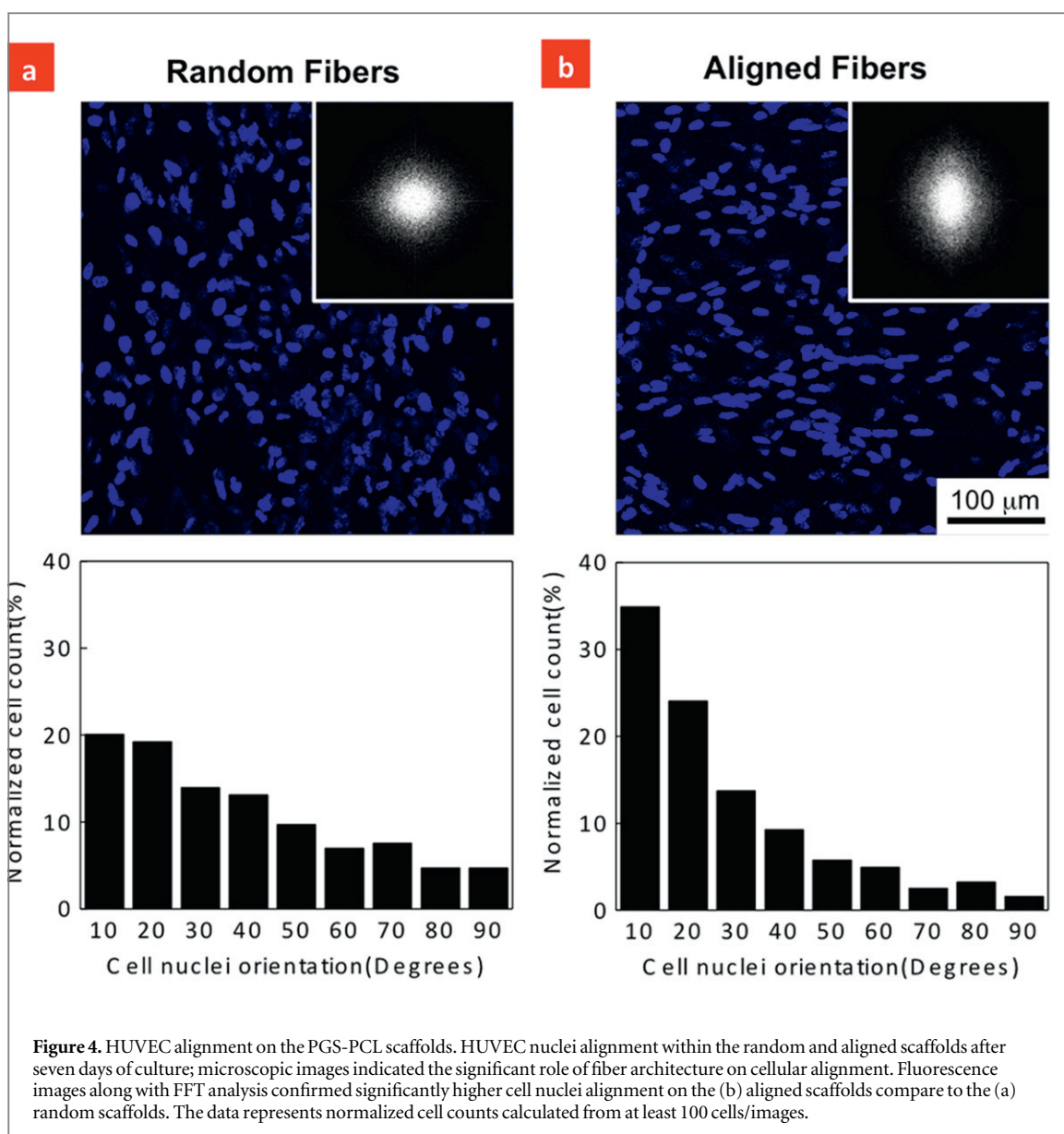
Previous studies by Zhang *et al* also confirmed similar growth behavior of human aortic endothelial cells on random silk nanofibrous scaffolds for 7 days of culture (Zhang *et al* 2008). Their studies demonstrated



that the cell proliferation was increased two folds on day 14 as compared to day 7. On the other hand, Heath *et al* reported a opposite finding showing that HUVECs seeded on randomly distributed hexyl methacrylate (HMA)/methyl methacrylate (MMA)/methacrylic acid (MAA) scaffolds with rubber-like material properties (elastic modulus $\sim 3 \pm 2$ MPa) and small pore area ($\sim 270 \pm 190 \mu\text{m}^2$) exhibited a significantly higher proliferation compared to the aligned scaffolds (Heath *et al* 2010). They concluded that that the pore size is a major factor in regulating proliferation and enzymatic activity of the cells. Therefore, we expect that the metabolic activity of HUVECs seeded on the aligned PGS-PCL scaffolds is governed by the material properties and structural characteristics of the scaffolds, by providing a coherent and unidirectional signaling in between the neighboring cells.

3.4. Cellular orientation on random and aligned scaffolds

To investigate the role of fiber orientation on cellular organization, nuclear alignment of HUVECs was quantified on the random and aligned scaffolds after 7 days of culture. As demonstrated in figures 4(a) and (b), fiber organization had a pronounced effect on the cell nuclear alignment. Specifically, on the aligned and random scaffolds, 35% ($n = 836$) and 20% of the cells ($n = 713$) were oriented within 10° of the preferred angle respectively. FFT analysis further confirmed nuclear alignment obtained through fluorescence images. To date, a large number of studies have demonstrated cellular alignment along the major axis of micro and nano-scale ridges, grooves, and micro-patterns; a phenomenon known as 'contact guidance' (Teixeira *et al* 2003, Curtis and Wilkinson 2001, Nikkhah *et al* 2012a). Contact guidance plays a



significant role in numerous biological processes such as cell migration (Clark *et al* 1990). In addition, cytoskeletal components including actin filaments as well as focal adhesion complexes are organized along with the direction of the features (Nikkhah *et al* 2012a, Gaharwar *et al* 2011). Therefore, similar process is expected to take place when endothelial cells are cultured on the PGS-PCL scaffolds. As the cells adhere on the aligned scaffolds, they probe and sense their local microenvironment through their integrin receptors and focal adhesion complexes. This ultimately results in reorganization of the cytoskeletal structure (i.e. actin filaments) of the cells and alters their morphology toward alignment and elongation along the fibers.

3.5. Effect of topography on cytoskeletal organizations

One of the major themes in vascularization is the development of biomaterials, which enable rapid

formation of cord-like structures. To date, several techniques have been developed to integrate vascularized networks within engineered tissue scaffolds (Kannan *et al* 2005, Lovett *et al* 2009, Khademhosseini and Langer 2007, Chen *et al* 2012). A number of these strategies are cell-based approaches where endothelial cells are incorporated within hydrogels and porous scaffolds to facilitate formation of capillary networks and cord-like structures (Nikkhah *et al* 2012b, Du *et al* 2011). In this regard, selection of a proper biomaterial plays a dominant role in the formation of functional vascularized networks. Herein, we investigated the role of fiber architecture on the formation of organized cellular structures.

Immunostaining demonstrated that the cells reorganized and formed a complex and aligned networks comprised of highly oriented actin fibers on the aligned scaffolds (figure 5(a)). The expressions of CD31, as a major determinant in angiogenesis (Newman *et al* 1990), was also investigated on the developed

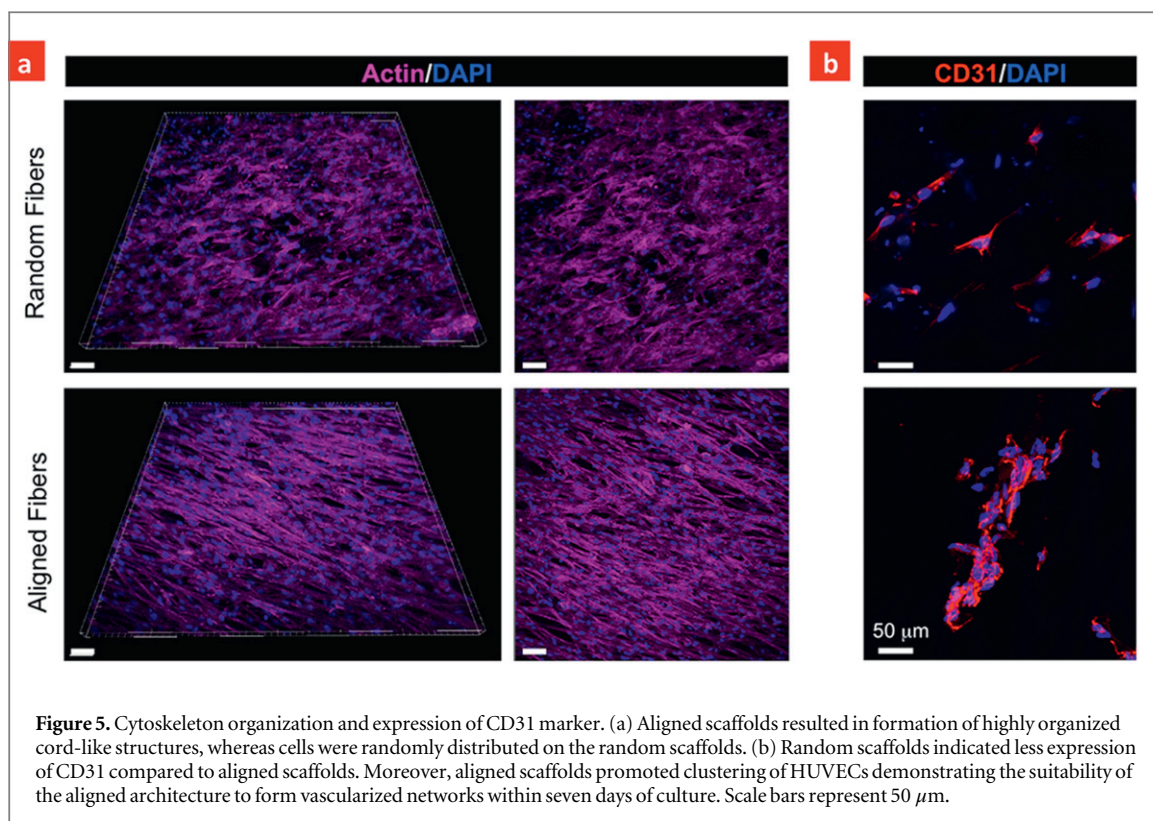


Figure 5. Cytoskeleton organization and expression of CD31 marker. (a) Aligned scaffolds resulted in formation of highly organized cord-like structures, whereas cells were randomly distributed on the random scaffolds. (b) Random scaffolds indicated less expression of CD31 compared to aligned scaffolds. Moreover, aligned scaffolds promoted clustering of HUVECs demonstrating the suitability of the aligned architecture to form vascularized networks within seven days of culture. Scale bars represent 50 μm .

scaffolds. Figure 5(b) indicates higher expression of CD-31 within the aligned scaffolds as compared to the random scaffolds. Although it is not clear if the fiber alignment resulted in enhanced CD-31 expression or the 3D microenvironment provided by electrospun scaffold played a major role. Specifically, CD-31 expression within clusters of cells was along the fiber directions demonstrating the importance of the aligned scaffolds for tissue engineering applications. Overall, our findings are in agreement with previous studies showing that electrospun scaffolds significantly affect morphology, proliferation and alignment of endothelial cells and can serve as suitable material to develop vascularized tissue constructs (Heath *et al* 2010, Zhang *et al* 2008). Furthermore, the developed scaffolds can be used a suitable biomaterials to enhance endothelial cells infiltration for potential applications in designing vascular graft.

Earlier reports have also highlighted the use of aligned scaffolds for tissue engineering (Yang *et al* 2005, Meng *et al* 2010, Xie *et al* 2010, Nguyen *et al* 2012, Tseng *et al* 2014). For example, our recent study on PGS-gelatin fibrous scaffold indicates that cardiomyocytes seeded on aligned scaffolds showed higher expression of sarcomeric α -actinin, Cx-43 and cardiac troponin I (Kharaziha *et al* 2013). In another study, mesenchymal progenitor cell were seeded on aligned and random scaffolds of poly(ester urethane) urea elastomer (Bashur *et al* 2009). They demonstrated that the fiber morphology and alignment play an important role on the expression of ligament

specific markers such as collagen 1 α 1, decorin, and tenomodulin. Thus, engineered PGS-PCL scaffolds may be used to engineer aligned tissue structures.

4. Conclusions

In this work, we investigated the effect of anisotropy of PGS-PCL scaffolds with variable mechanical properties on endothelial cell behavior. SEM images confirmed successful fabrication of aligned and random fibrous scaffolds. Uniaxial tensile test revealed higher elastic modulus of aligned scaffold as compared to the random scaffolds. Notably, aligned PGS-PCL scaffold enhanced cellular proliferation and organization and led to the formation of highly organized endothelial constructs as a necessary step for the development of vascularized tissue structures.

Acknowledgments

This research was funded by the US Army Engineer Research and Development Center, the Institute for Soldier Nanotechnology, the NIH (EB009196; DE019024; EB007249; HL099073; AR057837), and the National Science Foundation CAREER award (AK) SS acknowledges interdisciplinary training fellowship (NIH NRSA I32) awarded by System based Consortium for Organ Design and Engineering (SysCODE).

References

- Baker B M, Gee A O, Metter R B, Nathan A S, Marklein R A, Burdick J A and Mauck R L 2008 The potential to improve cell infiltration in composite fiber-aligned electrospun scaffolds by the selective removal of sacrificial fibers *Biomaterials* **29** 2348–58
- Bashur C A, Shaffer R D, Dahlgren L A, Guelcher S A and Goldstein A S 2009 Effect of fiber diameter and alignment of electrospun polyurethane meshes on mesenchymal progenitor cells *Tissue Eng. A* **15** 2435–45
- Bhardwaj N and Kundu S C 2010 Electrospinning: a fascinating fiber fabrication technique *Biotechnol. Adv.* **28** 325–47
- Bolgen N, Menceloglu Y Z, Acatay K, Vargel I and Piskin E 2005 *In vitro* and *in vivo* degradation of non-woven materials made of poly(epsilon-caprolactone) nanofibers prepared by electrospinning under different conditions *J. Biomater. Sci.-Polym. Ed.* **16**, pp 1537–55
- Cai W and Liu L 2008 Shape-memory effect of poly (glycerol–sebacate) elastomer *Mater. Lett.* **62** 2171–3
- Chen C S, Tan J and Tien J 2004 Mechanotransduction at cell-matrix and cell-cell contacts *Annu. Rev. Biomed. Eng.* **6** 275–302
- Chen Q, Liang S and Thouas G A 2011 Synthesis and characterisation of poly (glycerol sebacate)-co-lactic acid as surgical sealants *Soft Matter* **7** 6484–92
- Chen Q Z, Bismarck A, Hansen U, Junaid S, Tran M Q, Harding S E, Ali N N and Boccacini A R 2008 Characterisation of a soft elastomer poly (glycerol sebacate) designed to match the mechanical properties of myocardial tissue *Biomaterials* **29** 47–57
- Chen Y-C, Lin R-Z, Qi H, Yang Y, Bae H, Melero-Martin J M and Khademhosseini A 2012 Functional human vascular network generated in photocrosslinkable gelatin methacrylate hydrogels *Adv. Funct. Mater.* **22** 2027–39
- Clark P, Connolly P, Curtis A, Dow J and Wilkinson C 1990 Topographical control of cell behaviour: II. Multiple grooved substrata *Development* **108** 635–44
- Courtney T, Sacks M S, Stankus J, Guan J and Wagner W R 2006 Design and analysis of tissue engineering scaffolds that mimic soft tissue mechanical anisotropy *Biomaterials* **27** 3631–8
- Curtis A and Wilkinson C 2001 Nanotechnology and approaches in biotechnology *Trends Biotechnol.* **19** 97–101
- Dolatshahi-Pirouz A, Nikkha M, Gaharwar A K, Hashmi B, Guermani E, Aliabadi H, Camci-Unal G, Ferrante T, Foss M and Ingber D E 2014 A combinatorial cell-laden gel microarray for inducing osteogenic differentiation of human mesenchymal stem cells *Sci. Rep.* **4** 3896
- Du Y, Ghodousi M, Qi H, Haas N, Xiao W and Khademhosseini A 2011 Sequential assembly of cell-laden hydrogel constructs to engineer vascular-like microchannels *Biotechnol. Bioeng.* **108** 1693–703
- Engelmayr G C, Cheng M, Bettinger C J, Borenstein J T, Langer R and Freed L E 2008 Accordion-like honeycombs for tissue engineering of cardiac anisotropy *Nat. Mater.* **7** 1003–10
- Engler A J, Sen S, Sweeney H L and Discher D E 2006 Matrix elasticity directs stem cell lineage specification *Cell* **126** 677–89
- Fleischer S and Dvir T 2012 Tissue engineering on the nanoscale: lessons from the heart *Curr. Opin. Biotechnol.* **24** 664–71
- Gaharwar A K, Mihaila S M, Kulkarni A A, Patel A, Di Luca A, Reis R L, Gomes M E, van Blitterswijk C, Moroni L and Khademhosseini A 2014a Amphiphilic beads as depots for sustained drug release integrated into fibrillar scaffolds *J. Control. Release* **187** 66–73
- Gaharwar A K, Mukundan S, Karaca E, Dolatshahi-Pirouz A, Patel A, Rangarajan K, Mihaila S M, Iviglia G, Zhang H and Khademhosseini A 2014b Nanoclay-enriched poly (epsilon-caprolactone) electrospun scaffolds for osteogenic differentiation of human mesenchymal stem cells *Tissue Eng. A* **20** 2088–101
- Gaharwar A K, Schexnaider P J, Dundigalla A, White J D, Matos-Pérez C R, Cloud J L, Seifert S, Wilker J J and Schmidt G 2011 Highly extensible bio-nanocomposite fibers *Macromol. Rapid Commun.* **32** 50–7
- Hasan A, Memic A, Annabi N, Hossain M, Paul A, Dokmeci M R, Dehghani F and Khademhosseini A 2014 Electrospun scaffolds for tissue engineering of vascular grafts *Acta Biomater.* **10** 11–25
- Heath D E, Lannutti J J and Cooper S L 2010 Electrospun scaffold topography affects endothelial cell proliferation, metabolic activity, and morphology *J. Biomed. Mater. Res. A* **94** 1195–204
- Ifkovits J L, Devlin J J, Eng G, Martens T P, Vunjak-Novakovic G and Burdick J A 2009 Biodegradable fibrous scaffolds with tunable properties formed from photocross-linkable poly(glycerol sebacate) *ACS Appl. Mater. Interfaces* **1** 1878–86
- Jaafar I H, Ammar M M, Jedlicka S S, Pearson R A and Coulter J P 2010 Spectroscopic evaluation, thermal, and thermomechanical characterization of poly(glycerol-sebacate) with variations in curing temperatures and durations *J. Mater. Sci.* **45** 2525–9
- Kannan R Y, Salacinski H J, Sales K, Butler P and Seifalian A M 2005 The roles of tissue engineering and vascularisation in the development of micro-vascular networks: a review *Biomaterials* **26** 1857–75
- Kemppainen J M and Hollister S J 2010 Tailoring the mechanical properties of 3D-designed poly (glycerol sebacate) scaffolds for cartilage applications *J. Biomed. Mater. Res. A* **94** 9–18
- Khademhosseini A and Langer R 2007 Microengineered hydrogels for tissue engineering *Biomaterials* **28** 5087–92
- Khademhosseini A, Langer R, Borenstein J and Vacanti J P 2006 Microscale technologies for tissue engineering and biology *Proc. Natl. Acad. Sci.* **103** 2480–7
- Kharaziha M, Nikkha M, Shin S-R, Annabi N, Masoumi N, Gaharwar A K, Camci-Unal G and Khademhosseini A 2013 PGS: Gelatin nanofibrous scaffolds with tunable mechanical and structural properties for engineering cardiac tissues *Biomaterials* **34** 6355
- Kulangara K and Leong K W 2009 Substrate topography shapes cell function *Soft Matter* **5** 4072–6
- Lam C X F, Savalani M M, Teoh S-H and Hutmacher D W 2008 Dynamics of *in vitro* polymer degradation of polycaprolactone-based scaffolds: accelerated versus simulated physiological conditions *Biomed. Mater.* **3** 034108
- Liu Q Y, Tian M, Shi R, Zhang L Q, Chen D F and Tian W 2007 Structure and properties of thermoplastic poly(glycerol sebacate) elastomers originating from prepolymers with different molecular weights *J. Appl. Polym. Sci.* **104** 1131–7
- Lovett M, Lee K, Edwards A and Kaplan D L 2009 Vascularization strategies for tissue engineering *Tissue Eng. B* **15** 353–70
- Masoumi N, Johnson K L, Howell M C and Engelmayr G C Jr 2013 Valvular interstitial cell seeded poly(glycerol sebacate) scaffolds: toward a biomimetic *in vitro* model for heart valve tissue engineering *Acta Biomater.* **9** 5974–88
- Meng Z, Wang Y, Ma C, Zheng W, Li L and Zheng Y 2010 Electrospinning of PLGA/gelatin randomly-oriented and aligned nanofibers as potential scaffold in tissue engineering *Mater. Sci. Eng. C* **30** 1204–10
- Mihaila S M, Gaharwar A K, Reis R L, Marques A P, Gomes M E and Khademhosseini A 2013 Photocrosslinkable Kappa-Carrageenan hydrogels for tissue engineering applications *Adv. Healthcare Mater.* **2** 895–907
- Motlagh D, Yang J, Lui K Y, Webb A R and Ameer G A 2006 Hemocompatibility evaluation of poly (glycerol-sebacate) *in vitro* for vascular tissue engineering *Biomaterials* **27** 4315–24
- Newman P J, Berndt M C, Gorski J, White G C, Lyman S, Paddock C and Muller W A 1990 PECAM-1 (CD31) cloning and relation to adhesion molecules of the immunoglobulin gene superfamily *Science* **247** 1219–22
- Nguyen L T, Liao S, Chan C K and Ramakrishna S 2012 Enhanced osteogenic differentiation with 3D electrospun nanofibrous scaffolds *Nanomedicine* **7** 1561–75

- Nikkhah M, Edalat F, Manoucheri S and Khademhosseini A 2012a Engineering microscale topographies to control the cell–substrate interface *Biomaterials* **33** 5230–46
- Nikkhah M et al 2012b Directed endothelial cell morphogenesis in micropatterned gelatin methacrylate hydrogels *Biomaterials* **33** 9009
- Pritchard C D, Arnér K M, Langer R S and Ghosh F K 2010 Retinal transplantation using surface modified poly (glycerol-co-sebacic acid) membranes *Biomaterials* **31** 7978–84
- Rai R, Tallawi M, Grigore A and Boccaccini A R 2012 Synthesis, properties and biomedical applications of poly(glycerol sebacate) (PGS): a review *Prog. Polym. Sci.* **37** 1051–78
- Ravichandran R, Venugopal J R, Sundarrajan S, Mukherjee S and Ramakrishna S 2011 Poly (Glycerol sebacate)/gelatin core/shell fibrous structure for regeneration of myocardial infarction *Tissue Eng. A* **17** 1363–73
- Ravichandran R, Venugopal J R, Sundarrajan S, Mukherjee S, Sridhar R and Ramakrishna S 2012 Minimally invasive injectable short nanofibers of poly (glycerol sebacate) for cardiac tissue engineering *Nanotechnology* **23** 385102
- Sacks M S, Schoen F J and Mayer J E Jr 2009 Bioengineering challenges for heart valve tissue engineering *Annu. Rev. Biomed. Eng.* **11** 289–313
- Sant S, Coutinho D F, Sadr N, Reis R L and Khademhosseini A 2012 *Biomimetic Approaches for Biomaterials Development* (New York: Wiley) pp 471–93
- Sant S, Hwang C M, Lee S-H and Khademhosseini A 2011 Hybrid PGS–PCL microfibrillar scaffolds with improved mechanical and biological properties *J. Tissue Eng. Regen. Med.* **5** 283–91
- Sant S, Iyer D, Gaharwar A K, Patel A and Khademhosseini A 2013 Effect of biodegradation and de novo matrix synthesis on the mechanical properties of VIC-seeded PGS-PCL scaffolds *Acta Biomater.* **9** 5963–73
- Sohier J, Carubelli I, Sarathchandra P, Latif N, Chester A H and Yacoub M H 2014 The potential of anisotropic matrices as substrate for heart valve engineering *Biomaterials* **35** 1833–44
- Stevens M M and George J H 2005 Exploring and engineering the cell surface interface *Science* **310** 1135–8
- Sun Z J, Chen C, Sun M Z, Ai C H, Lu X L, Zheng Y F, Yang B F and Dong D L 2009 The application of poly (glycerol–sebacate) as biodegradable drug carrier *Biomaterials* **30** 5209–14
- Sun Z J, Sun C W, Sun B, Lu X L and Dong D L 2011 The polycondensing temperature rather than time determines the degradation and drug release of poly(Glycerol-Sebacate) doped with 5-fluorouracil *J. Biomater. Sci.-Polym. Ed.* **23** 833–41
- Sundback C A, Shyu J Y, Wang Y D, Faquin W C, Langer R S, Vacanti J P and Hadlock T A 2005 Biocompatibility analysis of poly(glycerol sebacate) as a nerve guide material *Biomaterials* **26** 5454–64
- Teixeira A I, Abrams G A, Bertics P J, Murphy C J and Nealey P F 2003 Epithelial contact guidance on well-defined micro- and nanostructured substrates *J. Cell Sci.* **116** 1881–92
- Tong Z, Sant S, Khademhosseini A and Jia X 2011 Controlling the fibroblastic differentiation of mesenchymal stem cells via the combination of fibrous scaffolds and connective tissue growth factor *Tissue Eng. A* **17** 2773–85
- Tseng H, Puperi D S, Kim E J, Ayoub S, Shah J V, Cuchiara M L, West J L and Grande-Allen K J 2014 Anisotropic poly (ethylene glycol)/polycaprolactone (PEG/PCL) hydrogel-fiber composites for heart valve tissue engineering *Tissue Eng.* **20** 2634–45
- Wagenseil J E and Mecham R P 2009 Vascular extracellular matrix and arterial mechanics *Physiol. Rev.* **89** 957–89
- Wang Y, Kim Y M and Langer R 2003 *In vivo* degradation characteristics of poly(glycerol sebacate) *J. Biomed. Mater. Res. A* **66A** 192–7
- Wang Y D, Ameer G A, Sheppard B J and Langer R 2002 A tough biodegradable elastomer *Nat. Biotechnology* **20** 602–6
- Xie J, Li X, Lipner J, Manning C N, Schwartz A G, Thomopoulos S and Xia Y 2010 ‘Aligned-to-random’ nanofiber scaffolds for mimicking the structure of the tendon-to-bone insertion site *Nanoscale* **2** 923–6
- Yang F, Murugan R, Wang S and Ramakrishna S 2005 Electrospinning of nano/micro scale poly (L-lactic acid) aligned fibers and their potential in neural tissue engineering *Biomaterials* **26** 2603–10
- Zhang H, Patel A, Gaharwar A K, Mihaila S M, Iviglia G, Mukundan S, Bae H, Yang H and Khademhosseini A 2013 Hyperbranched polyester hydrogels with controlled drug release and cell adhesion properties *Biomacromolecules* **14** 1299–310
- Zhang X, Baughman C B and Kaplan D L 2008 *In vitro* evaluation of electrospun silk fibroin scaffolds for vascular cell growth *Biomaterials* **29** 2217–27
- Zorlutuna P, Annabi N, Camci-Unal G, Nikkhah M, Cha J M, Nichol J W, Manbachi A, Bae H, Chen S and Khademhosseini A 2012 Microfabricated biomaterials for engineering 3D tissues *Adv. Mater.* **24** 1782–804